Arterial Wall Properties in Men and Women: Hemodynamic Analysis and Clinical Implications

19

John K.-J. Li

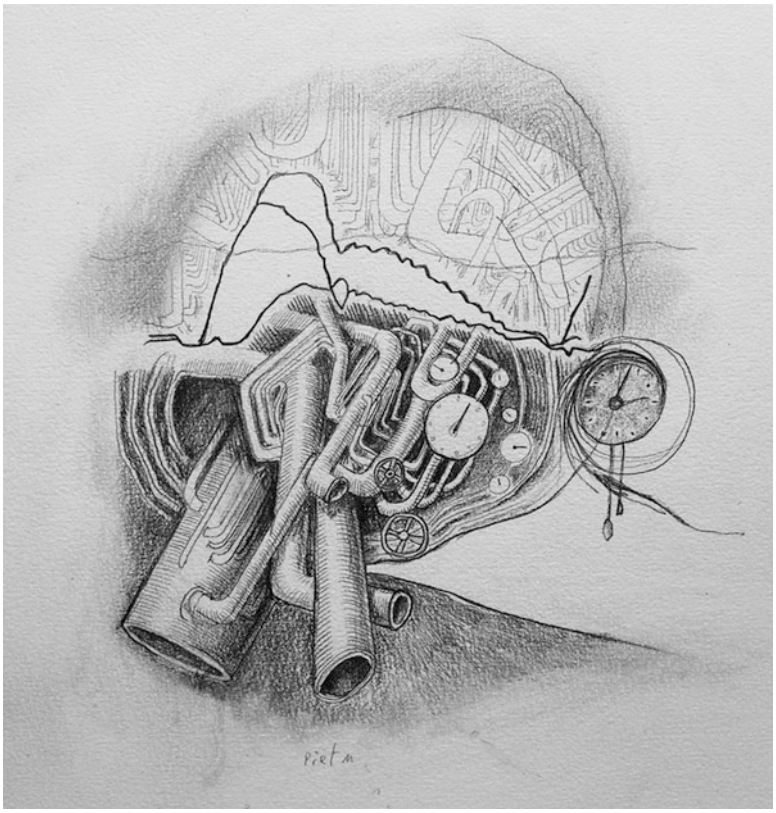

Arterial system with waveforms. Artwork by Piet Michiels, Leuven, Belgium.

J. K.-J. Li (✉)
Department of Biomedical Engineering, Rutgers University, Piscataway, NJ, USA
e-mail: johnkjli@soe.rutgers.edu

Abstract

The properties of arterial walls are dictated by their underlying structure, which is responsible for the adequate perfusion of conduit

P. L. M. Kerkhof, V. M. Miller (eds.), *Sex-Specific Analysis of Cardiovascular Function*,
Advances in Experimental Medicine and Biology 1065, https://doi.org/10.1007/978-3-319-77932-4_19

branching arteries and their vascular beds. Beginning with the mechanobiology of arteries in terms of their composition and individual contributions to overall viscoelastic behavior in men and women, pressure–flow relations are analyzed and noted in terms of sex differences. Hemodynamic function in terms of indices of vascular stiffness—such as pressure–strain elastic modulus, pulse wave velocity, augmentation index, and cardio–ankle vascular index—are evaluated. They all showed differences between the sexes, and these differences also were shown among people of different cultures. Recent studies also showed, in heart failure patients, a comparatively greater increase in peripheral resistance and a greater decreased arterial compliance in women. Wave separation into forward and reflected waves allows elucidation of mechanical and drug-treated similarities and differences in induced hypertension. This may provide insight into treatment strategy in terms of improving mechanobiology and designing drug therapy for the sexes. Finally, modeling studies are useful in identifying how arterial compliance and its pressure dependence can be better used in differentiating aging- and hypertension-induced changes that differentially affect the sexes.

Keywords
Vascular mechanics · Hemodynamic monitoring · Pulse waveform analysis · Arterial compliance · Mechanobiology · Sex differences

Introduction

Arteries and the Arterial System

Men are generally taller, heavier, and have a larger supporting frame structure than women. Their respective arterial systems function similarly in terms of the circulation of blood, but they are somewhat dissimilar in terms of geometric and viscoelastic properties. These dissimilarities contribute to differences in the pulsatile pressure and flow waveforms between the sexes. The root of the aorta begins at the aortic valve, the outlet of which is the ascending aorta, which has the largest diameter and overall compliance. The first arteries branching off the aorta are the left and right main coronary arteries. The aortic arch junction is formed by the ascending aorta, the brachiocephalic artery, the left subclavian artery and the descending thoracic aorta.

The descending thoracic aorta has numerous arterial branches coming off at almost right angles: For example, the segmental arteries perfuse the spinal cord, and the renal arteries perfuse the kidneys. The distal end of the descending aorta is the abdominal aorta, which forms the aorto-iliac bifurcation. The femoral arteries perfuse the upper thighs, and the tibial arteries perfuse the lower legs. The aorta has, comparatively speaking, the greatest geometric taper, with its diameter decreasing with increasing distance away from the ventricle. Both aortic length and diameter differ between the sexes. The common carotid arteries are the longest, most relatively uniform vessels with the least geometrical tapering [28]. The brachial arteries perfuse the upper arms leading to the distal radial arteries at the wrists. Carotid, femoral, brachial and radial arteries are the most common and accessible sites for noninvasive clinical blood pressure monitoring and, consequently, carotid-to-femoral and brachial-to-radial pulse wave velocity (PWV) measurements for assessing vascular stiffness, which will be discussed later in the text.

Structure of the Arterial Wall

Grossly speaking, the arterial wall consists of elastin, collagen and smooth muscle cells embedded in a mucopolysaccharide ground substance. A cross-sectional view reveals the tunica intima, which is the innermost layer consisting of a thin layer (0.5–1 μm) of endothelial cells, connective tissue and basement membrane. The middle layer is the thick tunica media, which is separated from the intima by a prominent layer of elastic tissue, in other words, the internal lamina. The media

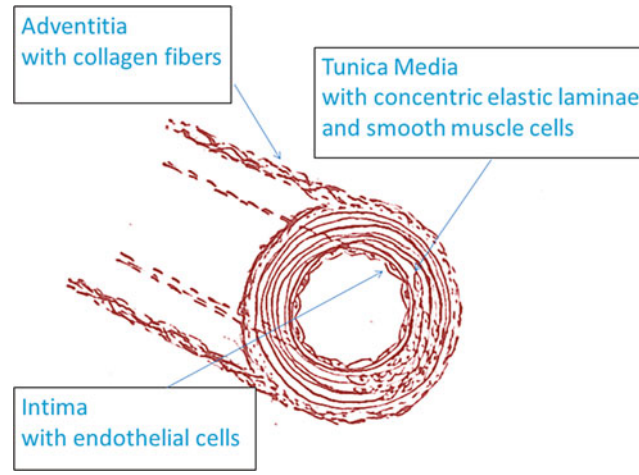

Fig. 19.1 Cross sections of the artery reveal three distinctive layers: the thin innermost tunica intima, the thick distensible tunica media, and the stiff outermost adventitia

contains elastin, smooth muscle cells and collagen fibers. The outermost layer is the adventitia, which is made up mostly of stiff, fibrous collagen. The difference in the wall composition separates arteries into large elastic arteries, such as the aorta, and smaller muscular arteries, such as the femoral and radial arteries.

Histological studies show that the elastic laminae are concentrically distributed and attached by smooth muscle cells and connective tissue (Fig. 19.1). In the longitudinal view, one can observe that the number of elastic laminae decreases with increasing distance from the aorta; however, the amount of smooth muscle increases, and the relative wall thickness increases. The wall thickness–to–radius ratio (h/r) is increased. The net stiffness is also increased, accounting for the increase in PWV toward the periphery as can be seen from the Moens-Korteweg formula relating propagating speed of the arterial pulse to conduit arterial elasticity and geometry [29]. The mechanical behavior of small peripheral arteries can be largely influenced by the behavior of the smooth muscle, particularly by the degree of its activation.

Gender-specific differences in aortic stiffness have been found between the sexes (e.g., [52]) and have been shown in the study of monkeys and rats [44]. In the latter study, elastin density decreased in male monkeys, and collagen increased significantly with aging in male and female rats. However, monkeys do not exhibit age-dependent increases in vascular diseases, such as hypertension, atherosclerosis and diabetes, observed in humans. Perhaps the relatively greater degree of acquired exercise and the low-fat diet (potassium-rich energy-generating banana is a favorite) indeed make a difference in monkeys. Generally, increased collagen and decreased elastin are associated with media thickening. Sex differences in the morphological structure of the tunica media of the human aorta have long been noted.

The extracellular matrix components, or those of elastin and collagen, govern the passive mechanical properties of the large and small arteries. Numerous studies exist on experimental animals and on humans [4, 51, 52]. Sex differences have also been reported. The contribution of smooth muscle to overall arterial wall properties and hemodynamic function has also been examined to a large extent. Smooth muscle activation becomes more important at greater blood pressures [3].

Mechanical Properties of Arteries

Vascular Stiffness and Arterial Wall Stress–Strain Relations

Arterial stiffness is traditionally expressed in terms of Young's modulus of elasticity, which gives a simple description of the elastic properties

of the arterial wall. Young's modulus of elasticity (E) is defined by the ratio of tensile stress (σ_t) to tensile strain (ε_t). When the relationship between stress and strain is a linear one, then the material is said to be "Hookean," or simply, it obeys Hooke's law of elasticity. This normally applies to a purely elastic material. It is only valid for application to a cylindrical blood vessel when the radial and longitudinal deformations are small compared with the respective lumen diameter or length of the arterial segment.

The arterial wall is anisotropic, consisting of various components exhibiting an intertwined elastic behavior. In diseased conditions, such as vascular hypertrophy and hypertension, selective thickening in the tunica media is often accompanied by an increase in collagen and a decrease in elastin and/or a change in the level of smooth muscle activation. These observed changes are not uniform throughout the arterial wall, in other words, they are anisotropic. Nevertheless, the assumption of isotropy allows simpler clinical quantitative descriptions of the mechanical behavior of the arterial wall properties and simplifies mathematical computation.

For a cylindrical isotropic arterial segment with radius r, wall thickness h and segment length 1, Young's modulus of elasticity in terms of tensile stress and tensile strain is:

$$E = \frac{\sigma_t}{\varepsilon_t} \tag{19.1}$$

Stress has the dimension of pressure or force (F) per unit area (A),

$$\sigma_t = \frac{F}{A} = P \tag{19.2}$$

where P is pressure.

Strain in the longitudinal direction, or along the length of the blood vessel, is expressed as the ratio of extension per unit length or the ratio of the amount stretched longitudinally to the length of the original vessel segment,

$$\varepsilon_t = \frac{\Delta l}{l} \tag{19.3}$$

Strain in the radial direction, or perpendicular to the vessel segment length, is the fraction of distention of the vessel lumen radius or diameter. It is given by:

$$\varepsilon_r = \frac{\Delta r}{r} \tag{19.4}$$

Changes in arterial wall thickness, h, often accompany radial changes. Detailed analysis of this aspect can be found elsewhere [29, 40]. When the arterial wall thickness, h, is considered, the relative volume (V) distensibility of the artery is given by:

$$\frac{1}{V}\frac{dV}{dP} = \frac{3rV}{2hE} \tag{19.5}$$

The magnitude of the h/r ratio separates arteries into "thin-walled" and "thick-walled" vessels. Thus, an increase in wall thickness or lumen radius alone can impact the overall distensibility of the artery. The consequence of this has been found to be particularly important in vascular hypertrophy. Thickening of the arterial wall is largely due to the remodeling in the tunica media.

Pressure–Strain Elastic Modulus

From the fractional change in pulsatile diameter, $\Delta D/D$, and the pulsatile change in pressure from systole to diastole or pulse pressure (PP), the difference between systolic (Ps) and diastolic (Pd) pressures, i.e., $\Delta P = Ps - Pd$, the pressure–strain elastic modulus (Ep) can be obtained, viz.:

$$Ep = \frac{\Delta P}{\left({}^{\Delta D}/_{D}\right)} \tag{19.6}$$

Thus, simultaneous recordings of pressure–diameter relations allow Ep to be readily computed. Figure 19.2 illustrates such recordings using ultrasonic dimension gages for recording aortic diameter and catheterization for recording aortic pressure.

In general, aortic diameters are larger in men than in women and have a greater PP through early adulthood. Ep is more commonly obtained

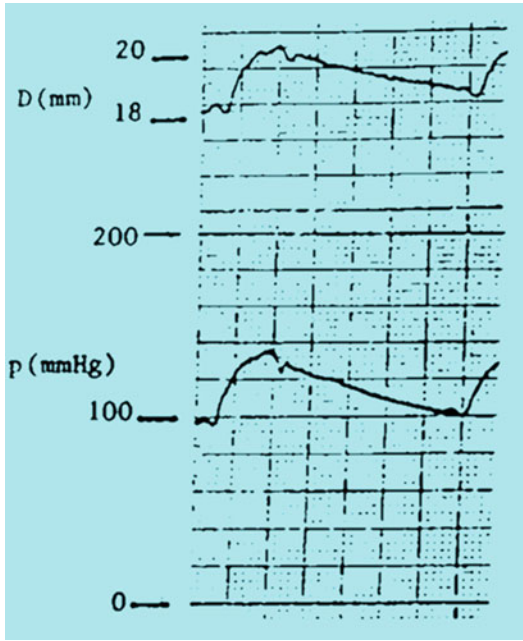

Fig. 19.2 Ultrasonic dimension gages were used to record the diameter of a dog aorta, together with aortic blood pressure, showing how Ep can be computed from the pressure–diameter relation $Ep = \mathrm{PP}/(\Delta D/D)$

noninvasively in the clinical setting with M-mode echocardiography for diameter measurement and brachial artery cuff for pulse pressure estimation.

To quantify the tension (T) exerted on the arterial wall due to intraluminal blood pressure distention, Laplace's law is useful. In the case of a blood vessel, there are two radii of curvature, one that is infinite in the longitudinal direction along the blood vessel axis and the other in the radial direction. Laplace's law is given as:

$$T = p \cdot r \tag{19.7}$$

This assumes the vessel has a thin wall or that the ratio of vessel wall thickness (h) to vessel lumen radius (r) is small, or $h/r \leq 1/10$. Here, p is the intramural–extramural pressure difference or the transmural pressure. When the vessel wall thickness is considered, the Lame equation is more relevant:

$$\sigma_t = \frac{pr}{h} \tag{19.8}$$

This relation is of particular importance in the analysis of an aneurysm, such as in abdominal aortic aneurysm (AAA) , where increased lumen radius is accompanied by decreased wall thickness such that a further increase in distending pressure can cause a rupture. In hypertension, however, T can be normalized by increasing the arterial wall thickness. Such chronical increase often leads to observed vascular hypertrophy.

To a good approximation, arteries are considered incompressible, with a Poisson ration of approximately 0.48. The Poisson ratio describes compressibility and is defined as the ratio of radial strain to longitudinal strain:

$$\sigma_n = \frac{\varepsilon_r}{\varepsilon_t} = \frac{\Delta r/r}{\Delta l/l} \tag{19.9}$$

When $\sigma_n = 0.5$, the material is said to be incompressible. This means that when a cylindrical artery is stretched, its volume remains unchanged.

Collagen is the stiffest wall component, with an Ep of 10^8–10^9 dynes/cm^2. This is some two orders of magnitude greater than those of elastin ($1–6 \times 10^6$ dynes/cm^2) and smooth muscle ($0.1–2.5 \times 10^6$ dynes/cm^2).

Elastin is relatively extensible, but it is not a purely Hookean material. In contrast, collagen is relatively inextensible because of its high elastic stiffness. Vascular smooth muscle can appreciably alter its elastic stiffness on activation. In addition, the mechanical properties of arterial vessel walls can be altered by neural mechanisms and by circulating catecholamines, such as norepinephrine. The overall composite of the arterial wall components operates in such a manner that elastin dominates the composite behavior at low pressures. At high pressures, collagen becomes more dominant. It has been found that Ep is a nonlinear function of pressure. The pressure dependence of the mechanical properties of arteries has been reported by several investigators (e.g., [3, 7, 36, 54]). With increasing positive transmural pressure, arterial vessel diameter is distended [53], while the corresponding compliance declines.

Longitudinally, along the arterial tree, we find that the number of elastic laminae decreases with increasing distance from the aorta, but the amount of smooth muscle increases and the wall

thickness–to–radius ratio (h/r) increases. Overall vascular stiffness is thus increased away from the heart [28]. This latter phenomenon accounts for the observed large increase in pulse wave velocity. A longitudinal section also reveals a helical organization of the collagen fiber network. This network contributes significantly to the anisotropic properties of the arterial wall.

Sex Differences in Arterial Wall Properties: Arterial Compliance and Distensibility

Sonesson et al. [47] examined sex and age differences in compliance and diameter of the human aorta. They defined compliance, given by

$$\mathrm{C} = \mathrm{dV}/\mathrm{dP}, \tag{19.10}$$

as the inverse of the *Ep* expressed as the PP obtained by auscultatory method to the corresponding fractional change in pulsatile diameter with respect to diastolic diameter, *Dd*.

$$Ep = \frac{\Delta P}{\left({}^{\Delta D}/_{Dd}\right)} \tag{19.11}$$

This definition differs from the conventional one when the mean diameter for the cardiac cycle is used for the denominator.

This group measured pulsatile diameter with an ultrasound echo-tracking device. They also calculated the arterial stiffness parameter based on a logarithmic relation between pressure and diameter for calculating a less pressure-dependent arterial compliance in vitro by Hayashi et al. [14] and modified for in vivo calculation by Kawasaki et al. [18], viz.:

$$\beta = \frac{\ln\left(\frac{Ps}{Pd}\right)}{\Delta D/Dd} \tag{19.12}$$

where Ps and Pd are systolic and diastolic pressures, respectively. Results showed that *Ep* and β are both greater in males than females for the abdominal aorta and that the differences increase significantly with age, exponentially in males and linearly in females. This may attribute to a comparatively lower blood pressure in women, but women have greater dilatation of the diameter with advancing age. The Ep-tracked stiffness parameter increases similarly.

This group [13] subsequently, using the similar technique, looked at the carotid artery in healthy adults. The pulsatile change in diameter was smaller with age, measuring from 12% to 14% greater in the young to just 5% greater in the elderly. The increase in peripheral resistance is slower than the decrease in arterial compliance as shown allometrically by Li et al. [32, 35].

A population-based study by van der Heijden-Spek et al. [50] showed differences in brachial arterial and aortic wall properties with advancing age and that such differences are sex dependent. They computed the distensibility coefficient as:

$$\mathrm{DC} = \left(\frac{\Delta A}{A}\right)/\Delta P \tag{19.13}$$

and compliance coefficient

$$\begin{aligned}\mathrm{CC} = \frac{\Delta A}{\Delta P} &= \left(\frac{\Delta V}{L}\right)/\Delta P \\ &= \pi\left(2D\cdot\Delta D + \Delta D^2\right)/4\Delta P\end{aligned} \tag{19.14}$$

Using the ultrasound echo-tracking device developed by themselves, Reneman's group [23] calculated DC and CC in the compliant aorta and muscular brachial artery and showed that, despite a larger brachial artery diameter and associated compliance in men, the distensibility was lower. With age, brachial artery dilatation is proportionally greater in women than in men, and brachial artery compliance did not decrease in men and increased in women. The opposite finding was found in the large compliant aorta, i.e., compliance decreased with increasing age in both sexes.

Hemodynamic Measurements and Model-Based Analysis of Arterial Wall Properties

The Windkessel Model

The idea of a lumped model of the arterial circulation was first described by Hales in 1733. Albeit

largely qualitative, he did emphasize the storage properties of large arteries and the dissipative nature of small peripheral resistance arteries. In his description, the blood ejected by the heart during systole into the arterial system distends the large arteries, primarily the aorta. During diastole, the elastic recoil of these same arteries propels blood to perfuse the smaller peripheral resistance vessels. This initiated the earlier conceptual understanding that the distensibility of large arteries is important in allowing the transformation of intermittent outflow of the heart to steady outflow throughout the peripheral arteries. In other words, the large overall "compliance" of the large arteries protects the stiff peripheral vessels of organ vascular beds from the large swing of blood pressure due to pulsations. The significance of arterial pulsations remains a topic of debate.

The Windkessel, or air-bellow, is now credited to Frank [11], the original intent of whom was to obtain stroke volume (SV) from the aortic pressure pulse (PP) contour or the so-called pressure-derived flow [24].

Relating Arterial Wall Properties to Pulsatile Pressure and Flow

The usefulness of the Windkessel model, shown in Fig. 19.3, is in its ability to quantify arterial compliance, C, and peripheral resistance, Rs, from hemodynamic pressure (P) and flow (Q) measurements.

The amount of blood flow, Q_s, stored in the elastic aorta during each contraction is the difference between ventricular ejection or inflow, Q_i, to the large distensible aorta and the outflow, Q_o, to the small peripheral muscular arteries,

$$Q_o = (P - P_v)/R_s \qquad (19.15)$$

The amount of outflow is equivalent to the pressure decrease from the arterial side (P) to the venous side (P_v) due to the peripheral resistance, R_s:

$$Q_o = (P - P_v)/R_s \qquad (19.16)$$

At steady flow, assuming that P_v is small, or $Pv = 0$, we obtain a familiar expression for estimating the total peripheral resistance, and with the total inflow, $Q = Q_i$,

$$R_s = \bar{P}/\bar{Q} \qquad (19.17)$$

or mean arterial pressure to mean arterial flow.

The storage property is described by arterial compliance, which expresses the amount of change in blood volume (dV) due to a change in distending pressure (dP) in the arterial lumen. In this case, we have

$$C = dV/dP \qquad (19.18)$$

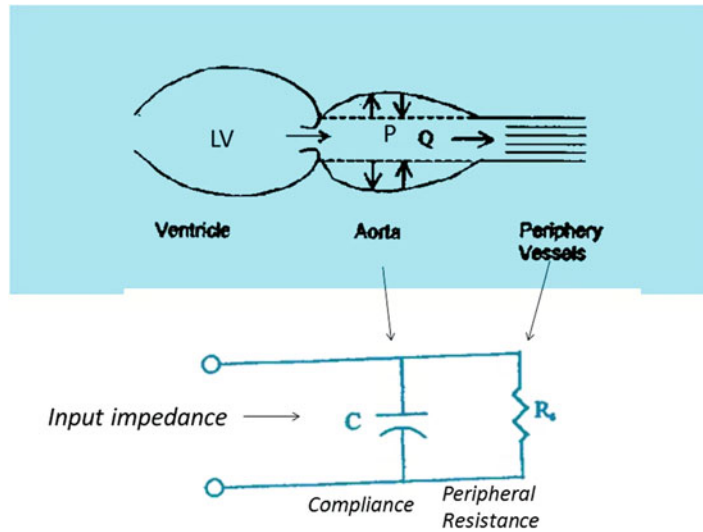

Fig. 19.3 Illustration of the left ventricle (LV) and the arterial circulation based on the two-element Windkessel model. The ventricle ejects into a compliant chamber representing the aorta; blood flow is stored in systole (solid line) and on diastolic elastic recoil (dotted line) stiff peripheral vessels are perfused. Compliance is represented by an energy-storing capacitor and the peripheral resistance by an energy-dissipating resistor

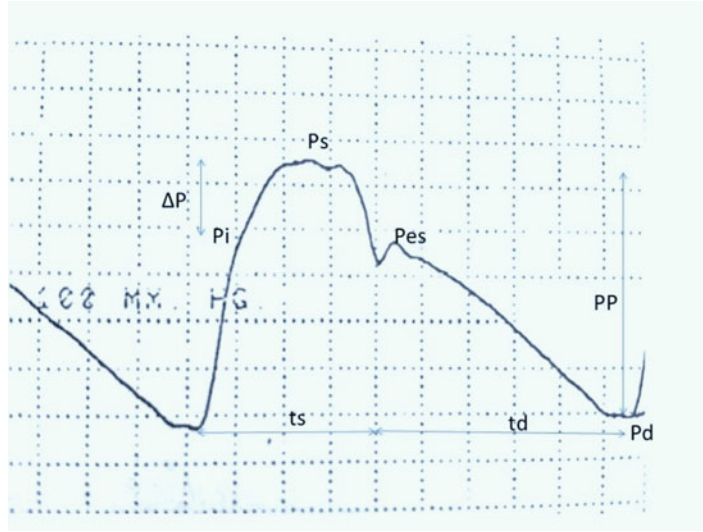

Fig. 19.4 Illustration of the measured aortic pressure pulse waveform for defining Ps, Pd, end-systolic pressure (Pes), PP (PP = Ps – Pd), inflection pressure (Pi) and augmented systolic pressure (ΔP = Ps − Pi)

For this reason, arterial compliance in the clinical setting has commonly been calculated from SV and PP, giving

$$C_v = SV/PP \tag{19.19}$$

The amount of blood flow stored, or Q_s, due to arterial compliance is related to the rate of change in pressure, which is pulsatile, in distending the artery,

$$Q_s = C\ dP/dt \tag{19.20}$$

Substituting for Q_s and Q_o, we obtain an expression relating the arterial pressure to flow incorporating the two Windkessel parameters, C and R_s:

$$Q(t) = Q_s + Q_o = C\ dP/dt + P/R_s \tag{19.21}$$

Thus, to express in words, total arterial inflow is the sum of the flow stored in the large compliant aorta in systole and the flow going into the stiff resistant periphery arteries during diastole.

In diastole, when inflow is zero after aortic valve closure, we have

$$0 = C\ dP/dt + P/R_s \tag{19.22}$$

or

$$dP/P = -dt/R_sC \tag{19.23}$$

Thus, the rate of diastolic aortic pressure decrease after aortic valve closure is dependent on both the compliance of the arterial system and its total peripheral resistance. If we integrate both sides, we have

$$\ln P = t/R_sC \tag{19.24}$$

or

$$P = P_o\ e^{-t/R_sC} \tag{19.25}$$

which is valid for the diastolic period or $t = t_d$.

The diastolic aortic pressure decay from Pes to Pd follows a mono-exponential manner with a time constant τ (Fig. 19.4).

$$P_d = P_{es}\ e^{-td/\tau} \tag{19.26}$$

The time constant of pressure decay, τ, which describes how fast the pressure falls, is determined by the product of resistance and compliance, viz.:

$$\tau = R_sC \tag{19.27}$$

thus giving total arterial compliance

$$C = \frac{t_d}{R_s \ln \frac{P_{es}}{P_d}} \tag{19.28}$$

An improved three-element Windkessel model (Fig. 19.5) of the arterial system, incorporating a characteristic impedance of the proximal aorta or Z_o, is now more widely used.

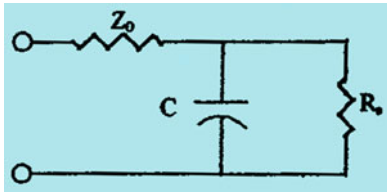

Fig. 19.5 An improved three-element Windkessel with Z_o representing the characteristic impedance of the proximal aorta

The Windkessel model compliance is determined in diastole only. Some investigators, such as Liu et al. [38], have used both the systolic and diastolic information contained in the pressure waveform and use the area method of calculating total arterial compliance:

$$C = \frac{DPTI/SV}{(SPTI + DPTI) \cdot PP} \tag{19.29}$$

where SPTI and DPTI are the systolic pressure–time integral and diastolic pressure–time integral, respectively.

Arterial Wall Properties Determined from Pulse Waveform Analysis

Pulse Wave Velocity

$$c_f = \frac{\Delta z}{\Delta t} \tag{19.30}$$

Pulse wave velocity has been popularly approximated by the so-called "foot-to-foot" velocity. Here, one simply estimates the pulse wave velocity (PVW) from the pulse transit time delay (PTT or Δt) of the "onset" or the "foot" between two pressure pulses measured at two different sites along an artery or the pulse propagation path. This requires, again, the simultaneous measurements of two pressures separated by a finite distance, Δz, normally 4–6 cm apart. A double-lumen catheter with two pressure ports connected to two pressure transducers or a Millar catheter with dual pressure sensors suffice for such measurement. The Moens-Korteweg formula relating PWV to stiffness is given by:

$$c_o = \sqrt{\frac{Eh}{2\rho r}} \tag{19.31}$$

where E is the Ep of the artery; h and r are the wall thickness and radius of the artery, respectively; and ρ is the density of blood. This formula is applicable to a single vessel, while foot-to-foot velocity has been obtained either for a single artery or over the pulse propagation path, e.g., over several arteries. Popular sites for noninvasive pulse wave velocity are the brachial, radial, carotid and femoral arteries. For instance, carotid-to-femoral pulse wave velocity has been used as an index of vascular stiffness change in the aorta as has carotid-to-radial pulse wave velocity (Fig. 19.6).

Wave Separation into Forward and Reflected Components

The amplification of pressure pulses has been attributed to the in-phase summation of reflected waves arising from structural and geometric nonuniformities. The microvascular beds have been recognized as the principal reflection sites. Thus, pulsatile pressure and flow waveforms contain information about the heart as well as the vascular system. Reflection in the vascular system has been suggested as a closed-end type because pressure is amplified and flow decreases, with arterioles being the major reflection site. By definition, reflected pressure and flow waves are 180° out of phase. This means an increase in reflection increases PP amplitude but decreases pulsatile flow amplitude.

Pressure (P) and flow (Q) waveforms measured at any site in the vascular system can be considered as the summation of a forward, or antegrade, traveling wave and a reflected, or retrograde, traveling wave:

$$P = P_f + P_r \tag{19.32}$$

$$Q = Q_f + Q_r \tag{19.33}$$

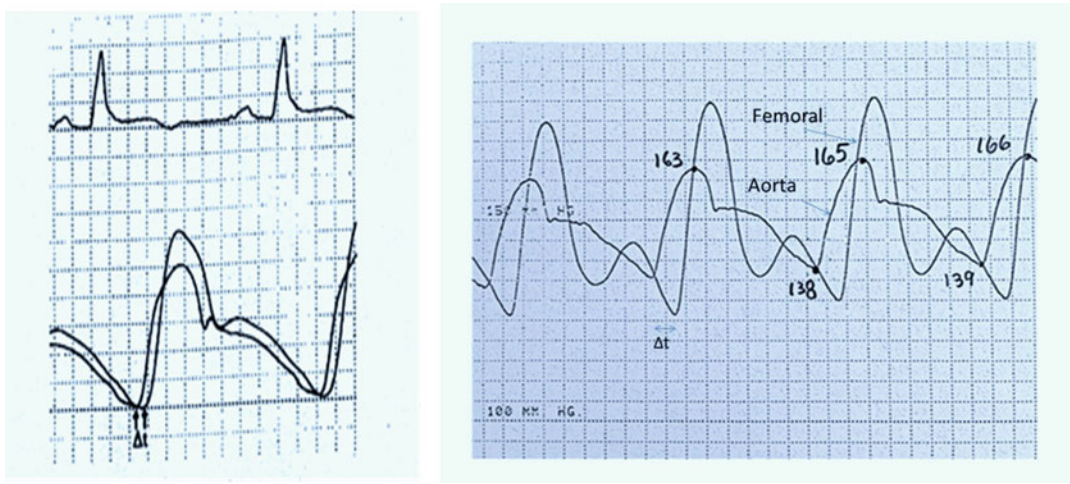

Fig. 19.6 PWV based on PTT (or Δt) of the onset of two pressures measured at a finite distance apart, in this case, those of the ascending and descending aortas (left panel). Pulse transit time delay is much more obvious when the two pressures are simultaneously measured at the ascending aorta and the femoral artery (right panel). Ps and Pd are displayed in this hypertensive subject. Femoral artery PP is significantly greater.

The forward and reflected pressure components can be resolved by means of the following set of equations:

$$P_f = (P + Q \cdot Zo)/2 \tag{19.34}$$

$$P_r = (P - Q \cdot Zo)/2 \tag{19.35}$$

where Z_o is the characteristic impedance, defined as the ratio of forward pressure to forward flow or, in other words, independent of wave reflections:

$$Z_o = \frac{P_f}{Q_f} = -\frac{P_r}{Q_r} \tag{19.36}$$

Z_o can be obtained from the average of the ratios of aortic pressure and flow during early systole when peripheral wave reflections exert minimal effect,

$$Zo = \frac{\Delta P}{\Delta Q} \tag{19.37}$$

or from the water-hammer formula,

$$Z_o = \frac{\rho c}{\pi r^2} \tag{19.38}$$

where ρ is the density of blood (1.06 g/cm^3), c is pulse wave velocity, and πr^2 is the cross-sectional area of the artery. The fast time-domain wave separation method by Li [28] is widely used.

Similarly, resolution of flow into its forward and reflected components (Fig. 19.7) can be obtained from a set of two equations:

$$Q_f = (Q + P/Z_o)/2 \tag{19.39}$$

$$Q_r = (Q - P/Z_o)/2 \tag{19.40}$$

Pulse pressure amplitude alone often does not indicate the underlying factors governing the morphology of blood pressure pulse waveforms. Thus, the routine clinically used cuff method for measuring Ps and Pd cannot be used to infer vascular stiffness or properties. One example is shown here in Fig. 19.8. Despite similar Ps and Pd induced either by a change in mechanical properties of the blood vessel wall or by a change in vasoactive states, the forward and reflected waveform morphologies and contributing factors differ [33]. A wave reflection-based distributed model [55] can be used to resolve the differences in vasoactive from mechanical factors.

The Augmentation Index and Transfer Function for Aortic Pressure Synthesis from Peripheral Pulse Tonometry

Because large-vessel properties can appreciably affect ventricular ejection, aortic compliance and

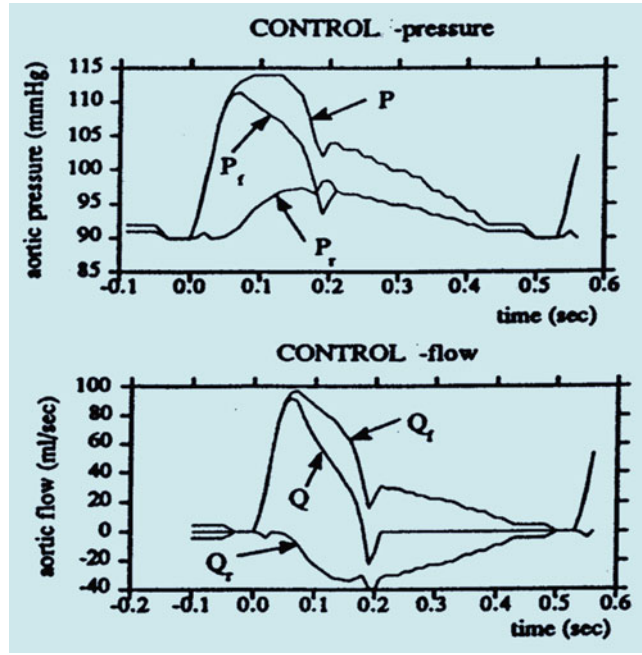

Fig. 19.7 Ascending aortic pressure, P, and flow, Q, separated into their respective forward (Pf, Qf) and reflected (Pr, Qr) components. Notice that wave reflection (+Pr and -Qr) has opposite effects on measured pressure and flow

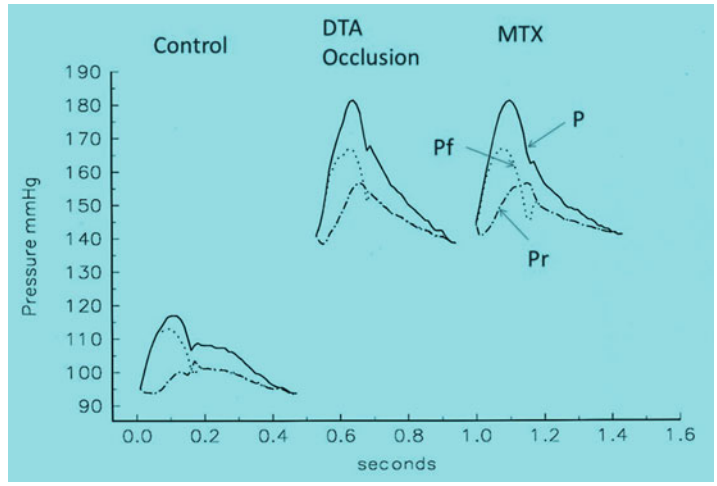

Fig. 19.8 Ascending aortic pressure and flow waveforms resolved into their respective forward (dotted line) and reflected (dash-dotted line) components during control (left), descending thoracic aorta (DTA) occlusion (center), and methoxamine-induced hypertension (MTX [right]). Although PPs are approximately the same due to mechanical (DTA) or vasoactive (MTX) interventions, the underlying morphology, mechanism, and forward and reflected waves differ

the wave reflections appearing in the aorta have become important markers for assessing arterial system behavior in the clinical setting. In addition, because frequency domain interpretation of wave reflections is complex and cumbersome to obtain, there exists a simplified index to interpret wave reflection in the aorta in the time domain. Ascending aortic pressure waveforms are defined in terms of their morphological differences and separated into different types. Peak Ps, Pd, PP, pressure at inflection point (P_i) where peak flow occurs, and augmented pressure (ΔP) are defined (see Fig. 19.4). Systolic pressure augmentation is given by:

$$\Delta P = P_s - P_i \tag{19.41}$$

and the corresponding augmentation index (AIx) for the aorta is given by

$$AIx = \frac{\Delta P}{PP} = \frac{P_s - P_i}{P_s - P_d} \tag{19.42}$$

Although simple to compute and widely used in the clinical setting to infer the amount of wave reflections or represent the reflection ratio, it is not equivalent to the reflection coefficient. The AIx is merely a single number and cannot represent the frequency content of the reflected wave, neither its timing nor its temporal amplitude. In addition, the inflection pressure is often obtained at the early upstroke of the systolic aortic pressure when fewer reflected waves are present. As we have seen previously, a significantly greater number of reflected waves occur in mid- to late systole. Thus, AIx in general underestimates the amount of wave reflections. This is clear when comparing AIx with the fundamental (first harmonic) reflection coefficient.

Noninvasive measurement is much preferred in the clinical setting. Since the central aortic pressure cannot be obtained noninvasively, it is generally derived from radial artery tonometry. Because radial artery is readily accessible and has the bone backing, the tonometry principle can be readily applied such that the applied pressure will equal the intravascular pressure when the circumferential stress is removed. This method obviously must rely on the skill of the investigator and subsequent interpretation of the recorded waveforms. A generalized built-in transfer function has been commonly used (e.g., [1, 17]). A more superior approach that is personalized, based on the Wiener system, has been recently proposed, and the results in human studies have shown significant improvement in estimating the central aortic pressure [41, 42].

Cyclic Variation of Arterial Compliance Within a Single Heart Beat

Given the differences in pulse pressure variations between the sexes, and because arterial compliance is pressure dependent, a more appropriate nonlinear model of the arterial system incorporating a pressure-dependent compliance element ($C(P)$) must be employed. This nonlinear model derived compliance-pressure loops are illustrated in Fig. 19.9 below [27, 30, 36]. The model consists of the characteristic impedance of the proximal aorta (Z_o), the peripheral resistance (Rs), and $C(P)$. The compliance is exponentially related to pressure and is expressed as

$$C(P) = a \cdot e^{b(P(t))} \tag{19.43}$$

where a and b are constants. The exponent b is normally negative. Thus, an inverse relationship is established between arterial compliance and blood pressure: with increasing blood pressure, arterial compliance decreases.

The compliance-pressure loop [27] constructed for each heart beat can be easily displayed as shown in Fig. 19.9 for varying

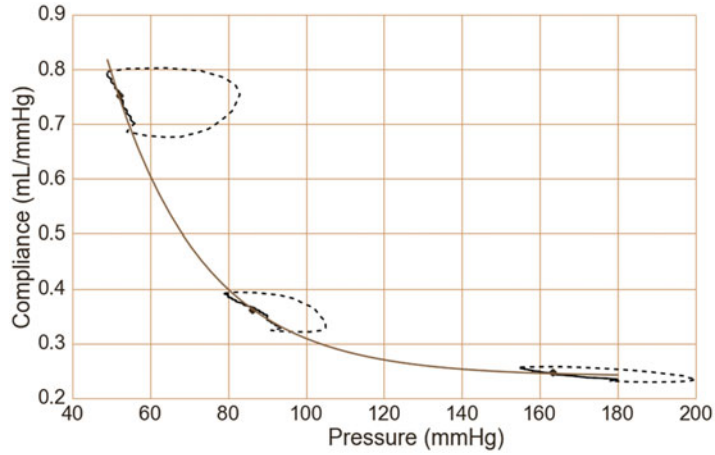

Fig. 19.9 Compliance versus pressure (solid line) and compliance-pressure loops (dotted lines) plotted for the control (middle), MTX-induced hypertension (right), and nitroprusside-induced vasodilation (left) cases (dog aorta). Note that overall compliance decreases with increasing pressure and that the loop area is compressed in hypertension and enlarged with a vasodilator

pressures. Very little work has been done in analyzing the beat-to-beat compliance-pressure relation for the sexes and the aging effects. It can be speculated, however, based on the $C(P)$ equation that the rate of change or the decrease in arterial compliance versus pressure (exponent b) is greater in elderly women. In addition, the beneficial effect of maximal arterial vasodilation-induced arterial compliance increment would be more limited than in their elderly male counterparts.

Sex Differences in Vascular Stiffness and Augmentation Index in Diseased Conditions

Abdominal Aortic Aneurym or AAA is among the more prominent cardiovascular disease and has been found to differentially affect the sexes, with lower prevalence but higher rupture rate in women than in men. Dobrin and Mrkvicka [6] have shown that depletion of elastin and collagen alters the tensile strength of the aorta and underlies the dilation of aneurysm. Analyzing wall properties by looking at the elastin synthesis and destruction in a small sample of men and women, Villard et al. [51] found that protein expression of elastin was less in women than men in cases of non-thrombolytic aneurysm.

It is well recognized that sex differences in vascular dysfunction exist, including differences in cardiovascular outcomes, particularly in relation to vascular stiffness (e.g., [9]). Women with end-stage renal disease (ESRD) have been suspected to have a higher mortality rate than men. Using the AIx for inferring systolic wave reflection and carotid-to-femoral artery pulse wave velocity as an index of vascular stiffness plus flow-mediated dilation (FMD) and velocity time integral (VTI) as a measure of microvascular endothelial function [8]. Guajardo et al. [12] investigated whether differences in vascular dysfunction lead to the different mortality differences in ESRD men and women because few studies have focused on sex-specific risk factors. Although they found little difference in pulse wave velocity, the AIx was significantly much greater in women than men. Mortality outcome was more associated with greater AIx and lower VTI and much less affected by PWV or FMD. Another interesting aspect is related to the Windkessel model parameters. In general, women have significantly decreased overall arterial compliance, C, and increased total peripheral resistance, Rs, than men. As such, the Windkessel time constant [i.e., $\tau = RsC = (1.32$ sec) vs. (0.97 sec)], as well as the τ/T ratio, is not significantly different because heart rates are similar.

Increased wave reflection and increased vascular stiffness both increase afterload to the heart, and are energeticlly wasterful [26, 28]. Hughes et al. [16] looked at whether their disproportional increase contributes to greater myocardial work in women. A generalized transfer function was used to derive aortic pressure from noninvasively measured radial arterial pressure.

Women in general have greater age-related increases in left ventricular mass (LVM) compared with men. This greater increased LVM leads to a greater oxygen demand and external work [25]. Our previous study also showed that women tend to experience what is known as "heart failure" with preserved ejection fraction, or HFpEF, which is associated with a greater incidence of diastolic dysfunction. The parallel or concurrent occurrence of LVM and hypertrophy with vascular hypertrophy has been reported [5]. Increased Ps in elderly women condition can be exacerbated by a ventricle with a double load [31].

Increased arterial stiffness associated with increased wave reflection, as evaluated by the AIx, has been reported in HFpEF patients. In a large community-based cohort study by Russo et al. [45], using a tonometer and 2D echocardiography, arterial stiffness and wave reflection were indirectly calculated based on PP/SV and total arterial compliance from the area method [38], AIx and PP amplification. AIx was based on the aortic pressure derived from a generalized transfer function. They showed that PP/SV stiffness and AIx were both greater and had a much lower total arterial compliance in women and that

these were related to their associated LV diastolic dysfunction. It should be noted here that this study was centered on the elderly with average age being more than 70 years, and the majority of the subjects were Hispanic and black, both of which tend to have greater incidences of hypertension. In addition, there were more female subjects with greater number exhibiting hypertension and obesity. The difference in the central aortic pressure AIx appears to differ between the sexes even in pre-pubescent children [48].

Consideration of the vascular load in terms of the LV–arterial system interaction has also been studied [2, 19, 20, 26, 34]. Because the ventricle is intimately connected to the ascending aorta, the central aortic pressure is of primary importance. In terms of the interaction, left ventricular and arterial elastances are generally computed to interpret the coupling and the extent of interaction of the LV and the arterial system. Our recent study [20] showed that in heart failure patients, the left ventricular end-systolic and end-diastolic volumes are significantly ($P < 0.034$ and $P < 0.016$, respectively) smaller in women ($N = 67$), while ejection fraction, LV maximum elastance, LV and arterial system coupling index, and mean arterial pressure and PP are greater ($P < 0.008$). These data showed that these female patients exhibit a greater increase in their peripheral resistances and a greater decrease in their arterial compliances compared with male patients.

Hayward and Kelly [15] showed sex differences in central arterial pressure waveforms, carotid to be specific, with more striking differences as age increases. Augmentation obtained was given by AIx (%) = −132 *Height (m) + 243, i.e., AIx is inversely proportional to height. Peaking in late Ps in elderly females led to a greater AIx. Females were found to have a shorter diastolic pressure–time integral. The subendocardial viability ratio in women, given as the ratio of DPTI/TTI. where TTI is tension–time index, a well-known index of myocardial oxygen consumption,

$$\mathrm{SEVR} = \mathrm{DPTI}/\mathrm{TTI} \qquad (19.44)$$

is significantly lower compared with male subjects despite similar TTI. However, sex differences in pulse wave reflection coefficients have been little studied because AIx cannot be fully related to the reflection coefficient. The latter is related to the whole cardiac cycle, while the former is only reflective of early systole [43, 55].

Hemodynamic Monitoring of Sex Differences in Different Cultures

In recent Korean studies [21, 22] looking at sex differences in arterial stiffness in middle-aged men and women, it was shown that aortic pulse wave velocity and brachial arterial pulse pressure amplification were both greater in men compared with women. Aortic PWV was assessed by carotid-to-femoral PWV as the common choice in the clinical setting. Radial artery tonometry–derived aortic AIx was obtained by way of transfer function. Pulse pressure amplification was obtained as the ratio of brachial arterial pressure to derived aortic pressure. Women have a greater AIx as shown by others. AIx was significantly correlated with age, Pd, and serum cholesterol levels.

Carotid-to-femoral PWV has been widely used as supposedly providing an indication of large-artery stiffness, i.e., of the aorta. It should be noted here that controversies exist because of the differing pulse transmission paths taken by the carotid and femoral arteries, in other words, opposite directions from the aortic arch junction.

A Chinese study by Liu et al. [37], based on radial artery monitoring, showed no difference between middle-aged men and women groups despite greater body weight and height in men. A Japanese study by Tomiyama et al. [49], using brachial–ankle pulse wave velocity (baPWV) as an index of vascular stiffness, showed that baPWV is greater in men than women. The difference, however, disappears when women reach menopause. This is attributed to the vasodilator effect of estrogen [10]. A study by Nishiwaki

et al. [39], using the cardio–ankle vascular index (CAVI) initially proposed by Shirai et al. [46], showed that CAVI increases with age, as expected, and is greater in men than in women.

References

1. Chen CH, Nevo E, Fetics B, Pak PH, Yin FC, Maughan WL, et al. Estimation of central aortic pressure waveform by mathematical transformation of radial tonometry pressure. Circulation. 1977;95:1827–36.
2. Coutinho T, Borlaug BA, Pellikka PA, Turner ST, Kullo IJ. Sex differences in arterial stiffness and ventricular-arterial interactions. J Am Coll Cardiol. 2013;61:96–103.
3. Cox RH. Arterial wall mechanics and composition and the effects of smooth muscle activation. Am J Physiol. 1975;229:807–12.
4. D'Armiento J. Decreased elastin in vessel walls puts the pressure on. J Clin Invest. 2003;112(9):1308–10.
5. Devereux RB, de Simone G, Ganau A, Koren MJ, Mensah GA, Roman MJ. Left ventricular hypertrophy and hypertension. Clin Exp Hypertens. 1993;15:1025–32.
6. Dobrin PB, Mrkvicka R. Failure of elastin or collagen as possible critical connective tissue alterations underlying aneurysmal dilatation. Cardiovasc Surg. 1994;2:484–8.
7. Drzewiecki G, Field S, Mubarak I, Li JK-J. Effect of vascular growth pattern on lumen area and compliance using a novel pressure-area model for collapsible vessels. Am J Physiol (Heart & Circ Physiol). 1997;273:H2030–43.
8. Dubin RF, Guajardo I, Ayer A, Mills C, Donovan C, Beussink L, et al. Associations of macro- and microvascular endothelial dysfunction with subclinical ventricular dysfunction in end-stage renal disease. Hypertension. 2016;68:913–20.
9. Duprez D, Jacobs DR Jr. Arterial stiffness and left ventricular diastolic function. Does sex matter? Hypertension. 2012;60:283–4.
10. Farhat MY, Lavigne MC, Ramwell PW. The vascular protective effects of estrogen. FASEB J. 1996;10:615–24.
11. Frank O. Die Grundform des arteriellen pulses. Z Biol. 1899;37:483–526.
12. Guajardo I, Ayer A, AD Johnson PG, Mills C, Donovan C, Scherzer R, et al. Sex differences in vascular dysfunction and cardiovascular outcomes: the cardiac, endothelial function, and arterial stiffness in ESRD (CERES) study. Hemodial Int. 2017;22:93. https://doi.org/10.1111/hdi.12544.
13. Hansen F, P Mangell B, Sonesson TL. Diameter and compliance in the human common carotid artery – variations with age and sex. Ultrasound Med Biol. 1995;21:l–9.
14. Hayashi K, Handa H, Nagasawa S, Okumura A, Moritake K. Stiffness and elastic behavior of human intracranial and extracranial arteries. J Biomech. 1980;13:175–84.
15. Hayward CS, Kelly RP. Gender-related differences in the central arterial pressure waveform. J Am Coll Cardiol. 1997;30:1863–71.
16. Hughes WE, Spartano NL, Lefferts WK, Augustine JA, Heffernan KS. Sex differences in noninvasive estimates of left ventricular pressure energetics but not myocardial oxygen demand in young adults. Artery Research. 2014;8:197–204.
17. Karamanoglu M, O'Rourke MF, Avolio AP, Kelly RP. An analysis of the relationship between central aortic and peripheral upper limb pressure waves in man. Euro Heart J. 1993;14:160–7.
18. Kawasaki T, Sasayama S, Yagi S, Asakawa T, Hirai T. Non-invasive assessment of the age related changes in stiffness of major branches of the human arteries. Cardiovasc Res. 1987;21:678–87.
19. Kerkhof PLM, Kresh JY, Li JK-J, Heyndrickx GR. Left ventricular volume regulation in heart failure with preserved ejection fraction. Physiol Report. 2013;1(2):1–10.
20. Kerkhof PLM, GR Heyndrickx, JK-J Li. Hemodynamic determinants and ventriculo-arterial coupling are sex-associated in heart failure patients. In: Proceeding of 38th annual international conference of the IEEE engineering in medicine and biology society, IEEE X-plore; 2016.
21. Kim H, Kim M, W Shim SO, Kim M, Park SM, Kim YH, et al. Sex difference in the association between brachial pulse pressure and coronary artery disease: the Korean women's chest pain registry (KoROSE). J Clin Hypertens (Greenwich). 2017;19:38–44.
22. Kim J, Park DS Kim JB, Kim KS, Jeong JW, Park JC, Oh BH, et al. On behalf of the KAAS investigators. Gender difference in arterial stiffness in a multicenter cross-sectional study: the Korean Arterial Aging Study (KAAS). Pulse. 2014;2:11–7.
23. Kool MJF, van Merode T, Reneman RS, Hoeks APG, Struijker Boudier HA. Evaluation of reproducibility of a vessel wall movement detector system for assessment of large artery properties. Cardiovasc Res. 1994;28:610–4.
24. Li JK-J. Pressure-derived flow: a new method. IEEE Trans Biomed Eng BME. 1983;30:244–6.
25. Li JK-J. Regional left ventricular mechanics during myocardial ischemia. In: Sideman S, editor. Simulation and modeling of the cardiac system. Boston: Martinus Nijhoff Publishers; 1987. p. 451–62.
26. Li JK-J. Feedback effects in heart-arterial system interaction. In: Sideman S, Beyar R, editors. Interactive phenomenon in the cardiac system. New York: Plenum; 1993. p. 325–33.
27. Li JK-J. A new description of arterial function: the compliance-pressure loop. Angiology. J Vascular Diseas. 1998;49:543–8.
28. Li JK-J. The arterial circulation: physical principles and clinical applications. New York: Springer; 2000.
29. Li JK-J. Dynamics of the vascular system. Singapore: World Scientific Publishers; 2004.
30. Li JK-J, Cui T, Drzewiecki G. A nonlinear model of the arterial system incorporating a pressure-dependent compliance. IEEE Trans Biomed Eng BME. 1990;37:673–8.
31. Li JK-J, Zhu JY, Nanna M. Computer modeling of the effects of aortic valve stenosis and arterial system afterload on left ventricular hypertrophy. Comput Biol Med. 1997;27:477–85.
32. Li JK-J, Zhu Y, O'Hara D, Khaw K. Allometric hemodynamic analysis of isolated systolic hypertension and aging. Cardiovasc Eng. 2007;7:135–9.
33. Li JK-J, Zhu Y, Geipel PS. Pulse pressure, arterial compliance and wave reflection under differential vasoactive and mechanical loading. Cardiovasc Eng. 2010;10:170–5.
34. Li JK-J, Atlas G. Left ventricle–arterial system interaction in heart failure. Clin Med Insight: Cardiol. 2015;9(Suppl 1):93–9. https://doi.org/10.4137/CMC.S18742.
35. Li JK-J, Zhu Y, Noordergraaf A. A comparative approach to analysis and modeling of cardiovascular function. Molecular, cellular, and tissue engineering. In: Bronzino JD, Peterson DR, editors. Biomedical engineering handbook, 4th ed. Chapter 26, pp26. London/New York: CRC Press/Boca Raton; 2015. p. 1–12.

36. Li JK-J, Zhu Y. Arterial compliance and its pressure dependence in hypertension and vasodilation. Angiology, J Vasc Diseas. 1994;45:113–7.
37. Liu C, Zhao L, Liu C. Effects of blood pressure and sex on the change of wave reflection: evidence from Gaussian fitting method for radial artery pressure waveform. PLoS One. 2014;9(11):e112895.
38. Liu Z, Brin KP, Yin FC. Estimation of total arterial compliance: an improved method and evaluation of current methods. Am J Phys. 1986;251:H588–600.
39. Nishiwaki M, Kurobe K, Kiuchi A, Nakamura T. N Matsumoto. Sex differences in flexibility-arterial stiffness relationship and its application for diagnosis of arterial stiffening: a cross-sectional observational study. PLoS One. 2014; https://doi.org/10.1371/journal.pone.0113646.
40. Noordergraaf A. Circulatory system dynamics. New York: Academic; 1978.
41. Patel A, Li JK-J. Aortic pressure estimation using blind identification approach on single input multiple output non-linear Wiener systems. IEEE Trans Biomed Eng. 2017a. https://doi.org/10.1109/TBME.2017.2688425
42. Patel A, Li JK-J. Validation of a novel nonlinear black box Wiener System model for arterial pulse transmission. Comput Biol Med. 2017b;88:11. https://doi.org/10.1016/j.compbiomed.2017.06.020.
43. Phan TS, Li JK-J, Segers P, Reddy-Koppula M, Akers SR, Kuna ST, et al. Aging is associated with an earlier arrival of reflected waves without a distal shift in reflection sites. J Am Heart Assoc. 2016;5:e003733. https://doi.org/10.1161/JAHA.116.003733.
44. Qiu H, Depre C, Ghosh K, Resuello RG, Natividad F, Rossi F, et al. Mechanism of gender-specific differences in aortic stiffness with aging in nonhuman primates. Circulation. 2007;116:669–76.
45. Russo C, Jin Z, Palmieri V, Homma S, Rundek T, Elkind MSV, et al. Arterial stiffness and wave reflection sex differences and relationship with left ventricular diastolic function. Hypertension. 2012;60:362–8.
46. Shirai K, Utino J, Otsuka K, Takata M. A novel blood pressure-independent arterial wall stiffness parameter; Cardio-Ankle Vascular Index (CAVI). J Atheroscler Thromb. 2006;13:101–7.
47. Sonesson B, Hansen F, Stale H, Lanne T. Compliance and diameter in the human abdominal aorta- the influence of age and sex. Eur J Vasc Surg. 1993;7:690–7.
48. Stoner L, Faulknera J, Westruppb N, Lambrick D. Sexual differences in central arterial wave reflection are evident in prepubescent children. J Hypertens. 2015;33:304–7.
49. Tomiyama H, Yamashina A, Arai T, Hirose K, Koji Y, et al. Influences of age and gender on results of noninvasive brachial-ankle pulse wave velocity measurement–a survey of 12517 subjects. Atherosclerosis. 2003;166:303–9.
50. Van der Heijden-Spek JJ, Staessen JA, Fagard RH, Hoeks AP, Struijker Boudier HA, Van Bortel LM. Effect of age on brachial Artery Wall properties differs from the aorta and is gender dependent. A population study. Hypertension. 2000;35:637–42.
51. Villard C, Eriksson P, Swedenborg J, Hultgren R. Differences in elastin and elastolytic enzymes between men and women with abdominal aortic aneurysm. Aorta. 2014;2:179–85.
52. Wagenseil JE, Mecham RP. Elastin in large artery stiffness and hypertension. J Cardiovas Translat Res. 2012;5:264–73.
53. Weizsacker H.W. and K. Pascal. Anisotropic passive properties of blood vessel walls. In: Cardiovascular system dynamics: models and measurements, pp. 347–362. Eds. T. Kenner, R. Busse, H. Hinghofer-Szalkay, Plenum, 1982.
54. Wells SM, Langeille BL, Adamson SL. In vivo and in vitro mechanical properties of the sheep in thoracic aorta in the perinatal period and adulthood. Am J Phys. 1998;274:H1749–60.
55. Zhang H, Li JK-J. A novel wave reflection model of the human arterial system. Cardiovasc Eng. 2009;9:39–48.